Composite Materials Based on Sodium Alginate and Synthetic Powders of Calcium Carbonate

Marat M. Akhmedov *, Tatiana V. Safronova, Arina A. Pavlova, Olga A. Kibardina, Tatiana B. Shatalova, Vadim B. Platonov, Albina M. Murashko, Yaroslav Y. Filippov, Egor A. Motorin, Olga T. Gavlina, Olga V. Boytsova, Anna Chirkova, Alexander V. Knotko, Natalya R. Kildeeva

Posted Date: 26 February 2026

doi: 10.20944/preprints202602.1618.v1

Keywords: vaterite; calcite; sodium alginate; cross-linking; composite

 doi:10.20944/preprints202602.1618.v1

Article

Composite Materials Based on Sodium Alginate and Synthetic Powders of Calcium Carbonate

Marat M. Akhmedov [1,*], Tatiana V. Safronova [2,3], Arina A. Pavlova [3], Olga A. Kibardina [3], Tatiana B. Shatalova [2,3], Vadim B. Platonov [2], Albina M. Murashko [3], Yaroslav Y. Filippov [3,4], Egor A. Motorin [3], Olga T. Gavlina [2], Olga V. Boitsova [2,3], Anna Chirkova [3], Alexander V. Knotko [3] and Natalia R. Kildeeva [1]

[1] Department of Chemistry and Technology of Polymer Materials and Nanocomposites, Kosygin Russian State University, Malaya Kaluzhskaya 1, 119071, Moscow, Russia

[2] Department of Chemistry, Lomonosov Moscow State University, Building, 3, Leninskie Gory, 1, 119991 Moscow, Russia

[3] Department of Materials Science, Lomonosov Moscow State University, Building, 73, Leninskie Gory, 1, 119991 Moscow, Russia

[4] Research Institute of Mechanics, Lomonosov Moscow State University, Building, 1, Michurinsky Pr., 119192 Moscow, Russia

* Correspondence: akhmedov.mm@yandex.ru

Abstract

Composite materials in form of granules, networks and films were created from suspensions of synthetic powders of calcium carbonates $CaCO_3$ in aqueous solutions of sodium alginate. Powders of calcium carbonates $CaCO_3$ were synthesized from 0.5M aqueous solutions of calcium chloride $CaCl_2$ and aqueous solutions of potassium K_2CO_3 (at molar ratio Ca/CO_3=1), sodium Na_2CO_3 (at molar ratio Ca/CO_3=1), ammonium $(NH_4)_2CO_3$ (at molar ratios Ca/CO_3=1 and Ca/CO_3=0.5) carbonates. Phase composition of powder synthesized from $CaCl_2$ and K_2CO_3 was presented by calcite. Phase composition of powders synthesized from other soluble carbonates included calcite and vaterite. The powder preparation protocol excluded the stage of by-product removing via synthesized powder washing providing their preservation at very low level. Presence of NH_4Cl as reaction by-product even in small quantities can be taken as a reason visually observed subsequences of cross-linking reaction at the stage of suspensions preparation. Aqueous solution of sodium alginate and suspensions containing powders synthesized from potassium K_2CO_3 and sodium Na_2CO_3 carbonates demonstrated the similar dependence of viscosities from share rate. Presence of $(NH_4)_2CO_3$ in the powder synthesized at molar ratio Ca/CO_3=0.5 was the reason of the lower viscosity of the suspension in comparison with suspensions loaded with powders containing KCl, NaCl and $(NH_4)_2Cl$ as reaction by-products due to decomposition of unstable $(NH_4)_2CO_3$ and gas phase formation. Presence of $(NH_4)_2Cl$ in the powder synthesized at molar ratio Ca/CO_3=1 in contrary was a reason of the highest viscosity suspension comparison with those under investigation. Granules, meshes and films were created via interaction of suspensions calcium carbonates $CaCO_3$ in aqueous solutions of sodium alginate with 0.25M aqueous solutions of calcium chloride $CaCl_2$ to provide formation of matrix of composites via Ca-crosslinking of sodium alginate followed by washing and freeze drying under deep vacuum. Created composite materials in form of granules, meshes and films based on Ca-cross-linked alginate and powders of synthetic calcium carbonate can be recommended for the skin wounds and bone defects treatment, and drug delivery carriers.

Keywords: vaterite; calcite; sodium alginate; cross-linking; composite

 doi:10.20944/preprints202602.1618.v1

1. Introduction

Composite materials with alginate matrices are wildly used not only in medicine [1–6] but also for environmental applications [7–9], as a semifinished items in the preparation of calcium phosphate granules [10] and as materials used for fruits storage [11]. Alginate is a naturally occurring polysaccharide extracted from brown algae, exhibiting ionic crosslinking capability that makes it an attractive biomaterial for various medical applications [12]. Its unique properties, such as biocompatibility, low toxicity, and ease of processing, have made it a popular choice for tissue engineering, wound healing applications due to their ability to promote cell growth, differentiation, and proliferation [13], and drug delivery systems [14–17]. Alginate-based biomaterials have been explored as a promising tool in regenerative medicine.

Alginate's ability to form hydrogels through ionic crosslinking with divalent cations like Ca^{2+} [10], Sr^{2+} [18], Mg^{2+} or Ba^{2+} [19], Zn^{2+} or Cu^{2+} [20] enables its use in creating scaffolds that mimic the extracellular matrix of tissues, promoting cell growth, differentiation, and proliferation [3]. Different ions Ca^{2+}, Sr^{2+}, Mg^{2+}, Ba^{2+}, Cu^{2+}, Fe^{3+} and Al^{3+} was systematically studied to investigate the relationship between ion concentration and cross-link density [21–23]. This property also allows alginate-based biomaterials to be used as carriers for drug delivery systems, providing a controlled release of therapeutic agents [24].

Alginate is widely used in its pure form or combined with other materials such as carbon-based nanoparticles, polymeric nanoparticles, metal or metal oxide nanoparticles and ceramic nanoparticles to create composite biomaterials [25]. These composites can be created using fillers of inorganic (metal oxides [26–28], calcium phosphates [29–35], carbonates [1,36,37] carbon nanotubes [38], calcium silicates [34]) and organic (collagen [39,40], polyester [41], cellulose [42], chitosan [43–45]) nature to enhance the mechanical properties and stability of alginate hydrogels, making them suitable for various applications, including biomedical.

The addition of calcium carbonate to alginate hydrogels creates composite materials with improved mechanical properties, stability and ability to adsorb different cations [37]. Currently, the most common materials for bone defect treating in clinical practice are calcium phosphates, in particular hydroxyapatite and tricalcium phosphate, due to their structural and chemical similarity to the mineral phase of bone [46]. However, calcium carbonate is a very promising alternative. It demonstrates excellent adsorption capacity in relation to proteins and growth factors, which additionally stimulates regenerative processes. The high surface area of calcium carbonate enhances the adsorption capacity of alginate-based composites, potentially improving drug-delivering capabilities over longer periods of time [47]. Calcium carbonate key advantages are a controlled rate of dissolution, ideally consistent with the rate of bone formation, high osteoconductivity and complete biocompatibility, since calcium and carbonate ions are natural metabolites of the body [48].

Calcium carbonate $CaCO_3$ has three modifications: calcite, aragonite and vaterite [49]. Hydrated [50,51] and amorphous forms [52] of $CaCO_3$ are also known. Calcium carbonate of different modifications can be synthesized by using different methods, including the liquid–liquid route and the solid–liquid–gas route [49,53,54] But the most convenient is the synthesis from solutions containing Ca^{2+} cation and CO_3^{2-} anion via precipitation [53,55]. Composites including calcite [56] preferably created for environmental applications with ability to adsorb different cations. Composites containing vaterite are preferably created for biomedical applications especially as drug delivery systems [47,57] mainly due to large specific surface area of powders consisting of sea urchin shaped particles [58]. An important aspect of practical application of different modification of calcium carbonate is the use as a filler of composite materials. Acting as a bioactive filler in a matrix of biopolymers, calcium carbonate makes it possible to create materials with programmable mechanical properties and resorption kinetics, combining the strength of ceramics and the elasticity of the polymer to maximize approximation to the characteristics of natural bone.

The aim of this investigation consisted in synthesis calcium carbonate powders from aqueous solutions of different pairs of precursors ($K_2CO_3/CaCl_2$, $Na_2CO_3/CaCl_2$, $(NH_4)_2CO_3/CaCl_2$,

 doi:10.20944/preprints202602.1618.v1

$2(NH_4)_2CO_3/CaCl_2$) and preparation of composite materials based on sodium alginate and synthetic powders of calcium carbonates in forms of films, meshes and granules.

2. Materials and Methods

2.1. Synthesis of $CaCO_3$ Powders

Calcium chloride $CaCl_2$ (CAS No. 10043-52-4, analytical pure grade, Rushim, Moscow, Russia), potassium carbonate K_2CO_3 (CAS No. 584-08-7, chemical pure grade, Rushim, Moscow, Russia) sodium carbonate Na_2CO_3 (CAS No. analytical pure grade, Rushim, Moscow, Russia), and ammonium carbonate $(NH_4)_2CO_3$ (CAS No. analytical pure grade, Rushim, Moscow, Russia) were used for the synthesis of powders.

The following reactions (1-3) were used to calculate the amounts of starting salts and expected both target and by-products:

$$K_2CO_3 + CaCl_2 \rightarrow CaCO_3 + 2KCl \quad (1)$$

$$Na_2CO_3 + CaCl_2 \rightarrow CaCO_3 + 2NaCl \quad (2)$$

$$(NH_4)_2CO_3 + CaCl_2 \rightarrow CaCO_3 + 2NH_4Cl \quad (3)$$

$$2(NH_4)_2CO_3 + CaCl_2 \rightarrow CaCO_3 + 2NH_4Cl + (NH_4)_2CO_3 \quad (4)$$

Labeling used for synthesized powders under investigation, quantities of initial salts for powders preparation are presented in Table 1.

Table 1. Conditions of powders' synthesis.

Labeling	Molar ratio CO_3^{2-}/Ca^{2+}	Starting salts and solutions							
		$CaCl_2$		K_2CO_3		Na_2CO_3		$(NH_4)_2CO_3$	
		C(M)xV(ml)	Mass, g	C(M)xV(ml)	Mass, g	C(M)xV(ml)	Mass, g	C(M)xV(ml)	Mass, g
CCK	1	0.5Mx400ml	22.2 g	0.5 Mx400ml	27.6 g	-		-	
CCNa	1	0.5Mx400ml	22.2 g	-		0.5Mx400ml	21.2 g	-	
CCNH4	1	0.5Mx400ml	22.2 g	-		-		0.5Mx400ml	19.2 g
CC2NH4	2	0.5Mx400ml	22.2 g	-		-		1.0Mx400ml	38.4 g

Quantities of expected target (**$CaCO_3$**) product and reaction by-products are presented in Table 2.

Table 2. Quantities of expected target (**$CaCO_3$**) product and reaction by-products.

Labeling	Molar ratio CO_3^{2-}/Ca^{2+}	Starting salts	Expected mass, g		
			$CaCO_3$	By-product	
			Mass, g	Composition	Mass, g
CCK	1	**$CaCl_2$ / K_2CO_3**	20.0	**KCl**	=0.4*74.6=29.8
CCNa	1	**$CaCl_2$ / Na_2CO_3**	20.0	**NaCl**	=0.4*58.46=23.4
CCNH4	1	**$CaCl_2$ / $(NH_4)_2CO_3$**	20.0	**NH_4Cl**	=0.4*53.5=21.4
CC2NH4	2	**$CaCl_2$ / $2(NH_4)_2CO_3$**	20.0	**NH_4Cl+$(NH_4)_2CO_3$**	=0.4*53.5+0.2*96.1=40.60

Four identical 0.5M aqueous solutions of calcium chloride were prepared. For preparation of 400 ml 0.5M solution of calcium chloride 22.2 g of anhydrous $CaCl_2$ was used. Four different aqua solutions of carbonates were prepared. For preparation of 400 ml of 0.5M solutions of different carbonates 27.6 g of potassium carbonate K_2CO_3, 21.2 r Na_2CO_3 of sodium carbonate and 19.2 g of ammonium carbonate $(NH_4)_2CO_3$ were used. 38.4 r $(NH_4)_2CO_3$ of ammonium carbonate $(NH_4)_2CO_3$ was used for preparation of 400 ml of 1M solution.

 doi:10.20944/preprints202602.1618.v1

Solution of $CaCl_2$ was added to the 0.5M solutions of K_2CO_3, Na_2CO_3, $(NH_4)_2CO_3$ and to the 1M solution of $(NH_4)_2CO_3$. The synthesis of each of the four powders was carried out in glass with a volume of 1 l at magnetic stirrer. Suspensions of precipitates were keeping under constant stirring during 60 min after addition of 400 ml of 0.5M solutions of $CaCl_2$ to the aqueous solutions of potassium, sodium or ammonium carbonates.

Prepared precipitates were separated from the mother liquors by vacuum filtration, placed in the plastic trays, evenly distributed over a large surface area and left to dry for 1 week. The powder preparation protocol excluded the stage of by-product removing via powder washing. Then powders were collected, weighted, crushed in an agate mortar and sieved through a polyester sieve with a mesh size of 200 microns. Transparent mother liquors were collected and dried for a month at 40 °C for water evacuation and crystallization of reaction by-products products solved in. The scheme of powders synthesis is presented at Figure 1.

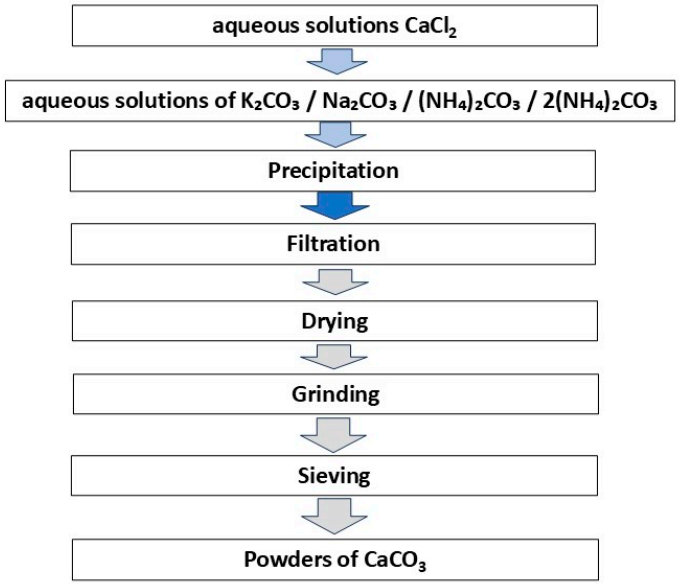

Figure 1. Scheme of $CaCO_3$ powders preparation.

The synthesized powders and isolated reaction by-products were weighed to determine their mass and to estimate the yield of synthesized powders and reaction by-products relatively to the theoretically possible amounts of expected target products and reaction by-product calculated in accordance with reactions (1-4) presented in Table 2

2.2. Preparation of Suspensions of Calcium Carbonate in an Aqueous Solution of Sodium Alginate

Sodium alginate E401 (Qingdao, Nanhan Yuanquan, Seaweed) and synthesized powders of $CaCO_3$ were used for preparation of suspensions of calcium carbonate in an aqueous solution of sodium alginate. Compositions of the suspensions of $CaCO_3$ in aqueous solution of sodium alginate are presented in Table 3 and Figure 2.

Table 3. Composition of the suspensions of $CaCO_3$ in an aqueous solution of sodium alginate.

Substances in suspensions	Mass of substances, g	Mass fraction, %
$CaCO_3$ (powder)	4	2.5
Sodium alginate (powder)	4	2.5
Distilled water	150	95

 doi:10.20944/preprints202602.1618.v1

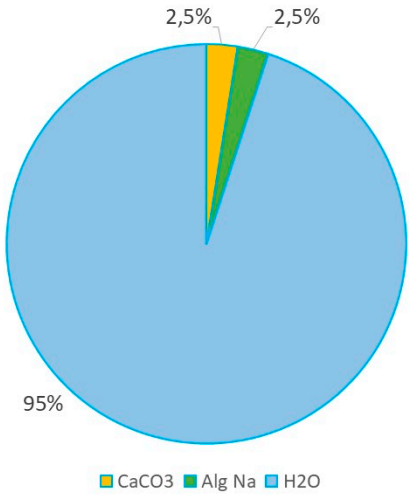

Figure 2. Composition of suspension of $CaCO_3$ in aqueous solution of sodium alginate.

To obtain composite suspensions containing particles of synthesized calcium carbonate, the following procedure was performed for each of the four powders obtained. 150 ml of distilled water was placed in to the 250 ml volume glass. 4.0 g of synthesized calcium carbonate was added to the 150 ml of distilled water. The resulting aqueous suspension was stirred on a magnetic stirrer for 30 minutes. Then, 4.0 g of sodium alginate was added in small portions to the prepared aqueous suspension of calcium carbonate under constant stirring. After adding the entire mass of sodium alginate, mixing was continued for 30 minutes to ensure complete dissolution of the polymer chains and the formation of a homogeneous, highly viscous dispersed system. The resulting thick, viscous suspensions were passed through a sieve with a mesh size of 100-200 microns to eliminate possible large aggregates and ensure maximum uniformity. The procedure was performed manually using a spatula. Labeling of prepared composite suspensions consisted of short name of polymer used (AlgNa) and labeling of powder used as a filler, i.e.
AlgNa_CCK, AlgNa_CCNa, AlgNa_CCNH4, AlgNa_CC2NH4.

2.3. Preparation of Samples of Composite Materials from Suspensions of Calcium Carbonate in an Aqueous Solution of Sodium Alginate

Preparation of samples of composite granules, films and meshes from suspensions of synthesized powders $CaCO_3$ in aqueous solution of sodium alginate via cross-linking in 0.25M aqueous solution of $CaCl_2$ was done according scheme presented at Figure 3.

An aqueous solution of calcium chloride ($CaCl_2$) with a concentration of 0.25 M was prepared to be used as cross-linking agent for sodium alginate according to the ion crosslinking reaction (5):

$$2(C_6H_7O_6Na)_n + nCaCl_2 \rightarrow nCa(C_6H_7O_6)_2 + 2nNaCl, \text{ где } (C_6H_7O_6Na) \qquad (5)$$

To prepare granules 50 ml syringes were filled with the suspension of synthesized powders of calcium carbonate in aqueous solution of sodium alginate. Holding the syringe at a height of 3-5 cm from the surface of the 20-30 ml of 0.25M aqueous solution of $CaCl_2$, the suspensions were squeezed drop by drop into it. Upon contact of each drop with the $CaCl_2$ solution, an instant gelification (crosslinking) of the surface occurred with the formation of granules. After molding, the granules were kept in 0.25M aqueous solution of $CaCl_2$ for 30 minutes to complete the gelation process throughout the volume. About 30 granules were obtained from aqueous solution of sodium alginate and from suspensions of synthesized powders of calcium carbonate in aqueous solution of sodium alginate.

 doi:10.20944/preprints202602.1618.v1

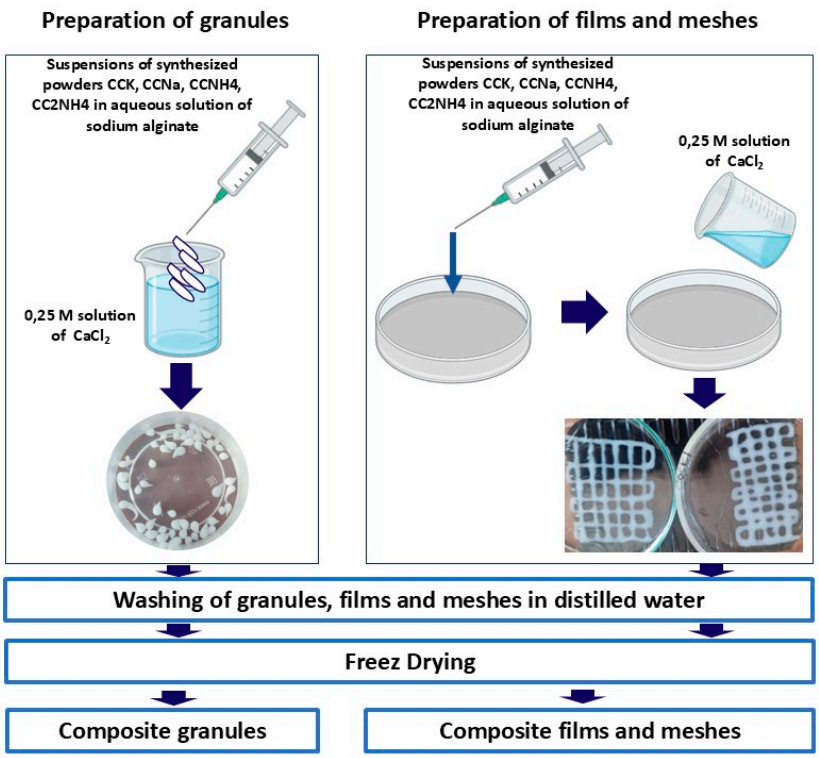

Figure 3. Scheme of composite granules, films and meshes preparation via cross-linking in 0.25M aqua solution of $CaCl_2$.

To prepare pattern in the form of a grid or lattice suspension of synthesized powder of calcium carbonate in aqueous solution of sodium alginate was randomly squeezed out of a syringe with a thin needle onto the bottom of a glass Petri dish, forming a pattern in the form of a grid or lattice. Pattern in the form of rectangular film was obtained by extruding the suspension of synthesized powder of calcium carbonate in aqueous solution of sodium alginate and spreading it with a flat surface of a spatula to obtain a layer of uniform thickness.

Immediately after forming, the resulting meshes and films were carefully covered with a prepared 0.25 M solution of $CaCl_2$ to initiate crosslinking. The samples were also kept in solution for 30 minutes.

After the crosslinking was completed, all the obtained samples (granules, meshes, films) were removed from the solution, washed with distilled water to remove excess $CaCl_2$ and NaCl (by-product of reaction (5)) from the surface and cryogenically dried.

Photos of prepared samples of granules, meshes, films are presented at the Figure 4. Labeling of prepared samples consisted of short name of polymer matrix (AlgCa) and labeling of powder used as a filler.

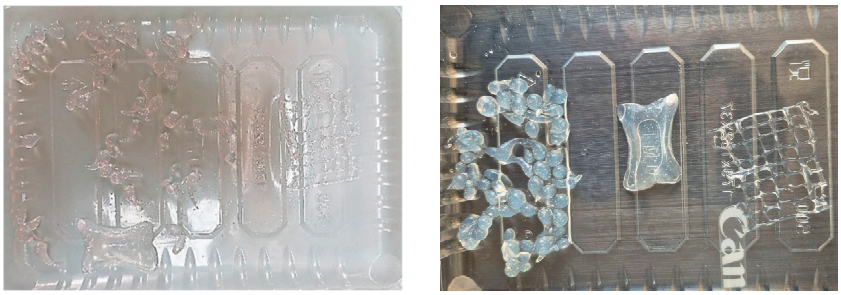

AlgCa

 doi:10.20944/preprints202602.1618.v1

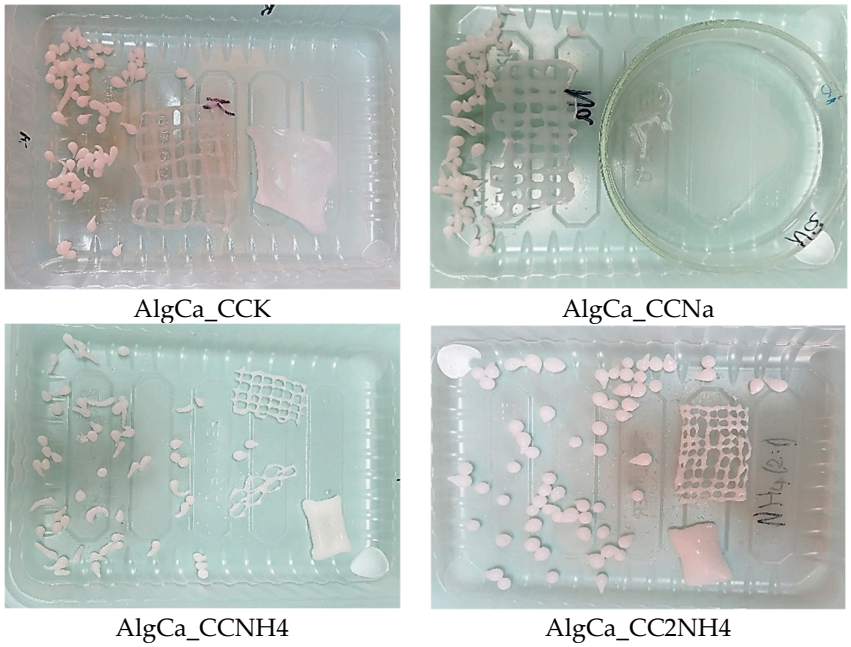

Figure 4. Photos of prepared composites with Ca-cross-linked alginate matrix loaded with synthetic powders of $CaCO_3$.

2.4. Methods of Analysis

The phase composition of synthesized powders and composites was studied by X-ray powder diffraction (XRD) analysis using CuKα radiation (λ = 1.5418 Å, step 2θ – 0.02°) using Rigaku D/Max-2500 diffractometers (Rigaku Corporation, Tokyo, Japan) in the angle range 2θ = 2...70° or Tongda TD-3700 (Dandong Tongda Science & Technology Co., Ltd., Dandong, China) in the angle range 2θ = 3...70°. The X-ray patterns were analyzed using the WinXPOW program and the ICDD PDF-2 (http://www.icdd.com/products/pdf2.htm, accessed on 10 February 2026) [59] databases and the Match! program. (https://www.crystalimpact.com/, accessed on 10 February 2026). The quantitative ratio of the target phases in the synthesized powders was determined using the Match!3 program, https://www.crystalimpact.com/.

FTIR-spectra of powders after synthesis and drying and composites were recorded in the transmission mode in the wavenumbers range of 4000–400 cm^{-1} with a step of 4 cm^{-1} on a Perkin Elmer Frontier spectrometer (Perkin Elmer, Waltham, Massachusetts, USA). The survey was carried out with potassium bromide tablets (7 mm diameter) containing 1 mass% of the test sample. The tablets were prepared by carefully grinding KBr together with the sample, followed by pressing into tablets at a pressure of 50 bar.

The particle size distributions for powder samples were determined by laser diffraction in an aqueous medium using a Fritsch Analysette-22 instrument (Fritsch GmbH, Idar-Oberstein, Germany). Photos of meshes were done using Nexcope NSZ818 stereo microscope (Ningbo Yongxin Optics Co., Ltd. (Novel Optics), China).

Scanning electron microscopy (SEM) images of the synthesized powders were characterized using an NVision 40 microscope (Carl Zeiss, Jena, Germany) in secondary electron imaging mode (SE2 detector). SEM images of the surfaces of composites were studied using a scanning electron microscope with an auto emission source JEOL JSM-6000PLUS Neoscope II (JEOL Ltd., Tokyo, Japan). For the study, the samples were glued onto a copper substrate using carbon tape, and a layer of gold ~15 nm was sprayed. The survey was carried out in vacuum mode. The accelerating voltage of the electron gun was up to 5 kV. The images were obtained in secondary electrons at magnifications up to 1000× and recorded in digitized form on a computer.

 doi:10.20944/preprints202602.1618.v1

Thermal analysis (TA) including thermogravimetry (TG) and differential thermal analysis (DTA) of synthesized powders and composites was performed using an NETZSCH STA 409 PC Luxx thermal analyzer (NETZSCH, Selb, Germany) during heating in air (10 °C/min, 40–1000 °C), the specimen mass being at least 10 mg. The gas-phase composition was monitored by a QMS 403C Aëolos quadrupole mass spectrometer (NETZSCH, Selb, Germany) coupled with a NETZSCH STA 409 PC Luxx thermal analyzer (NETZSCH, Selb, Germany). The mass spectra were registered for the following m/Z values: 18 (H_2O); 44 (CO_2).

To calculate bulk density of suspensions mass of 2 ml was weighed. The viscosity of suspensions and aqueous solutions of sodium alginate in a rotary stationary (CSR) mode was studied using an Anton Paar MCR 302e modular rheometer (Anton Paar GmbH, Austria) in a cylinder-to-cylinder geometry (cell volume 1 ml) in the shear rate range from 1 to 100 s^{-1}. The measurements were carried out at a room temperature of 23 °C.

Indirect investigation of properties of suspensions of calcium carbonate in an aqueous solution of sodium alginate via drying at room temperature. For an indirect assessment of viscosity, we considered the spreading area of the same mass of suspensions. 10.44 g of each suspension were dosed onto the flat surface of a glass Petri dish (Figure 5).

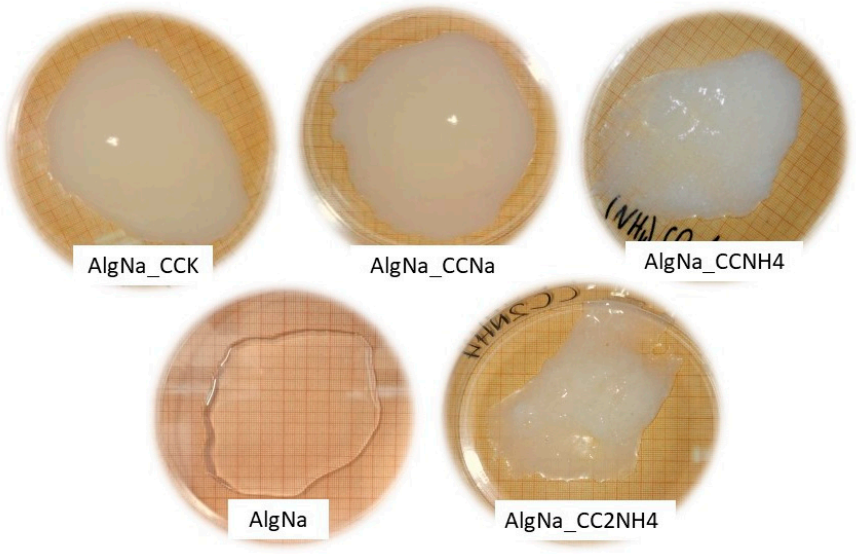

Figure 5. Photos of suspension after dosing them onto the flat surface of a glass Petri dish and the spreading stopped.

The sample was allowed to flow freely until an equilibrium state was reached and the spreading stopped. After stabilization of the spreading spot, a quantitative assessment of its area was carried out. Dimensions of suspensions area as an indirect characteristic of the ability to spread were estimated visually using millimeter paper after about 15 min after placing them on the glass surface. To do this, measurements of the linear dimensions of the formed spot were carried out using the applied millimeter paper, followed by the calculation of its area. Photos of suspension are shown at Figure 5. Mass changing of these suspensions during drying at room temperature were controlled by weighting. Investigation of properties of suspensions of calcium carbonate $CaCO_3$ in an aqueous solution of sodium alginate was done according scheme presented at Figure 6.

 doi:10.20944/preprints202602.1618.v1

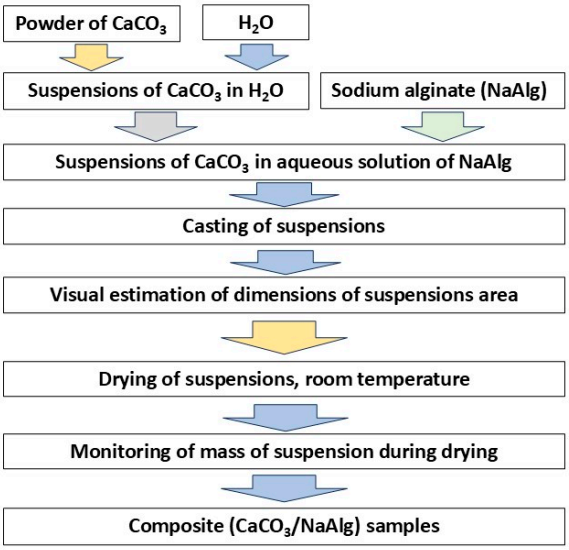

Figure 6. Scheme of indirect investigation of properties of suspensions of calcium carbonate in an aqueous solution of sodium alginate via drying at room temperature.

3. Results and Discussion

Phase composition of prepared powders presented at Figure 7. Phase composition of powder CCK synthesized from $CaCl_2$ and K_2CO_3 according XRD data was presented by calcite. Phase composition of powders (CCNa, CCNH4, CC2NH4) synthesized from other soluble carbonates included calcite and vaterite. The powder preparation protocol excluded the stage of by-product removing via powder washing providing their preservation at very low level. Never the less it is impossible to see any reflexes of reaction by-product (see reactions (1)-(4)) such as KCl, NaCl, NH_4Cl or $NH_4Cl+(NH_4)_2CO_3$ taken in excess. The main reason for using excess of $(NH_4)_2CO_3$ consisted in well known fact that presence of NH_4^+ ions facilitates formation of thermodynamically unstable phase of vaterite. Addition reason for using excess of $(NH_4)_2CO_3$ consisted in the intention to compensate for the volatile nature of ammonium carbonate.

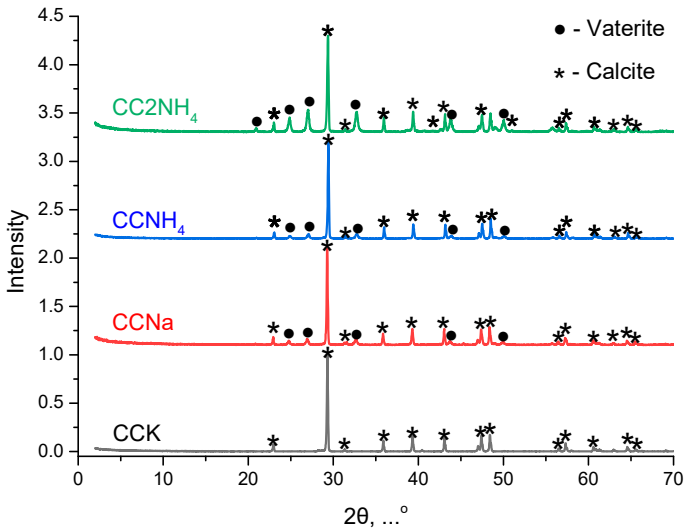

Figure 7. XRD data of powders after synthesis: •— vaterite (PDF No 33-268; No 96-900-7476); * —calcite (PDF No 5-586; No 96-900-0096).

 doi:10.20944/preprints202602.1618.v1

Estimation of quantity (wt. %) of different phases presented in synthesized powder can be seen ay Figure 8. Quantities of vaterite are not very high and increases in the row CCNa, CCNH4, CC2NH4 of synthesized powders. Presence of NH_4^+ in the reaction zone can be taken as a factor contributing to the higher content of vaterite phase. But basic pH of aqueous solutions of soluble carbonates used can be taken as factor providing preferable calcite as thermodynamically stable phase formation.

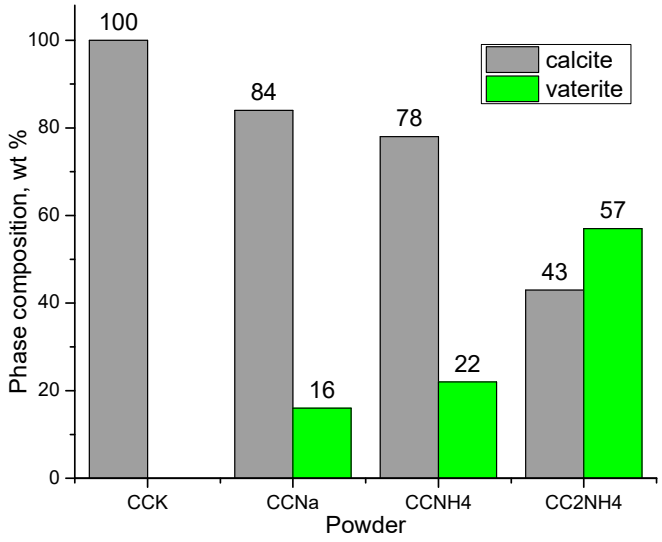

Figure 8. Phase composition of synthesized powders. Calculation was made using Match! (Card numbers for calcite No 96-900-0096 and for vaterite No 96-900-7476).

The masses of the synthesized $CaCO_3$ powders after filtration and drying and collected by-products are presented in Table 3. The yield of $CaCO_3$ can be estimated as high, close to the theoretically possible. The same conclusion can be done about masses of collected by-products for powders CCK, CCNa, CCNH4. Low yield of by-product for CC2NH4 when $(NH_4)_2CO_3$ was taken in excess can be explained by the low stability of this carbonate.

Table 3. The masses of the synthesized $CaCO_3$ powders and collected by-products.

Labeling	Synthesized powder of $CaCO_3$			By-product			
	Expected mass, g	Collected mass, g	The yield, %	Composition	Expected mass, g	Collected mass, g	The yield, %
CCK	20.0	18.8	94.0	KCl	29.8	28.5	95.6
CCNa	20.0	19.8	99.2	NaCl	23.4	21.9	93.7
CCNH4	20.0	19.5	97.7	NH_4Cl	21.4	19.2	89.6
CC2NH4	20.0	20.1	100.3	NH_4Cl+$(NH_4)_2CO_3$	40.6	25.1	61.9

FTIR spectra of synthesized powders are presented at Figure 7. No vibrations of vaterite can be found for powder CCK. Vibrations both of calcite and vaterite can be found in the FTIR spectra for powders CCNa, CCNH4, CC2NH4. So, the conclusion can be done that data of XRD and FTIR analysis are in the agreement.

 doi:10.20944/preprints202602.1618.v1

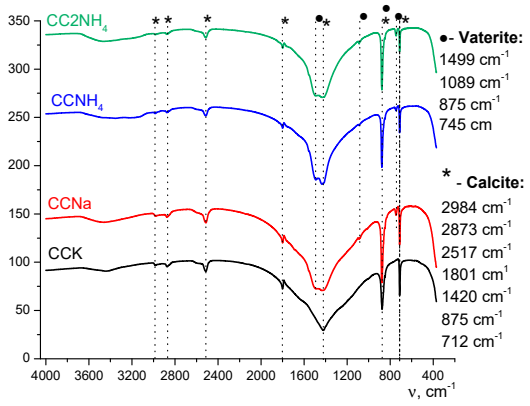

Figure 7. FTIR spectra of synthesized powders.

The spectrum of the CCK powder demonstrates characteristic bands corresponding exclusively to calcite modification. In particular, the splitting of valence carbonate ion vibrations typical of calcite is observed in the range of ~712 cm^{-1} and ~875 cm^{-1}, as well as a doublet of deformation vibrations in the range of about 1400-1500 cm^{-1}, which is a consequence of a decrease in the symmetry of the carbonate ion in the crystal lattice of rhombohedral calcite. The absence of a single sharp band in the spectrum in the region of ~745 cm^{-1}, which is a diagnostic sign of vaterite, unambiguously indicates its absence in this sample.

On the contrary, the FTIR spectra of all other powders (CCNa, CCNH4, CC2NH4) show a complex composition indicating a mixture of polymorphic phases. Along with the bands inherent in calcite, an absorption band unique to hexagonal vaterite at ~745 cm -1, corresponding to the valence vibrations of the carbonate ion, is clearly identified in these spectra. In addition, there is a change in the shape and position of the bands in the region of ~875 cm^{-1} and ~1100 cm^{-1}, which is also a consequence of the superposition of the vibrational spectra of two different crystalline phases. The combination of these spectral features unequivocally confirms the presence of both calcite and vaterite in these samples.

Thus, FTIR spectroscopy, being sensitive to the local environment and the symmetry of the carbonate ion in the crystal lattice, serves as a reliable independent method that is fully consistent with X-ray phase analysis. Both methods unequivocally indicate that selective formation of stable calcite occurs only in a powder CCK, while in all other cases crystallization proceeds through the stage of formation of metastable vaterite, which is preserved in the final product.

Particle size distribution of synthesized powders presented in Figure 8.

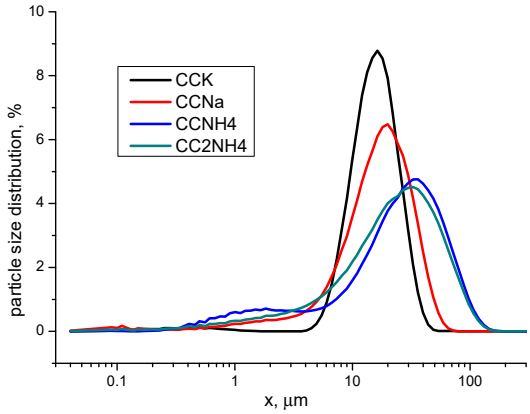

Figure 8. Particle size distributions in powders prepared.

 doi:10.20944/preprints202602.1618.v1

Dimensions of particles (aggregates of individual crystals) in CCK powder are in the interval 4.4-50.1 μm with the maximum distribution peak at 16.5 μm. Dimensions of particles in CCNa powder are in the broader interval 0.6-74.5 μm with the maximum distribution peak at 19.6 μm. Particles size distribution in CCNH4 and CC2NH4 powders practically have no difference. Dimensions of particles for these powders are in the interval 0.3-170.3 μm with the maximum distribution peak at 34.7 μm (CCNH4) and 31.2 μm (CC2NH4). The more quantity of the particles of vaterite phase the broader interval of particles (aggregates of individual crystals) dimensions. The reason of broader interval of particles distribution for powders CCNH4 and CC2NH4 can be explained with the special sea urchin shaped particles of vaterite having the ability to cling to each other. More over presented in powders reaction by-product even in the low quantity can play a binging role to keep individual crystals in the aggregated particles.

SEM images of synthesized powders are presented at Figure 9. Powder CCK (Figure 9, a, b) consisted of particle of prismatic shape which is characteristic for modification of calcite. Powders CCNa (Figure 9, c, d), CCNH4 (Figure 9, e, f), and CC2NH4 (Figure 9, g, h) consisted of particle both of prismatic shape and sea urchin shaped particles which is characteristic for modification of vaterite.

TA data presented at the Figures 10 (TG) and 11 (MS for m/z=44). The total mass loss for powders CCK and CCNa was 46.0%. The total mass loss for powders CCNH4 and CC2NH4 was 49.6% and 49.0% respectively.

$$CaCO_3 \rightarrow CaO + CO_2 \quad (6)$$

It worth to note that $CaCO_3$ decomposition stared for all powder at about 600 °C (Figure 11). And this process finished at different temperatures for different powders: 855 °C (CCK), 830 °C (CCNa), 820 °C (CCNH4) and 785 °C (CC2NH4).

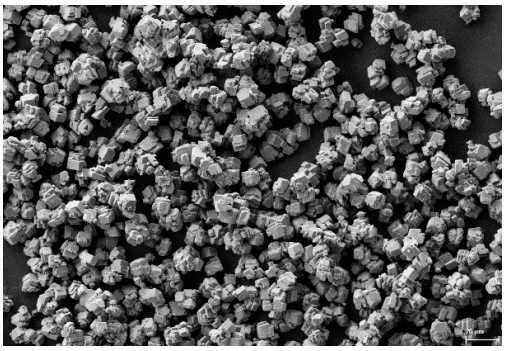

(a) CCK

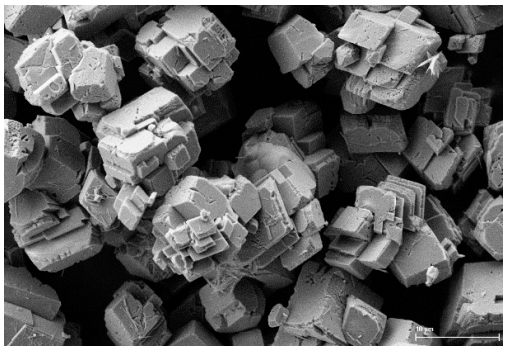

(b) CCK

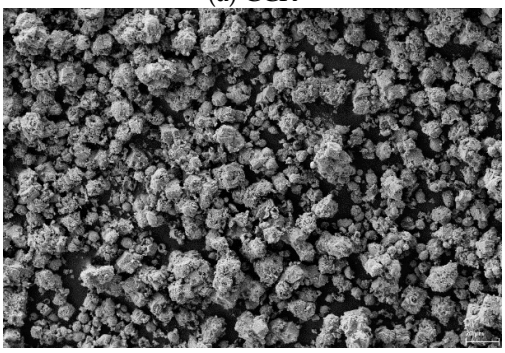

(c) CCNa

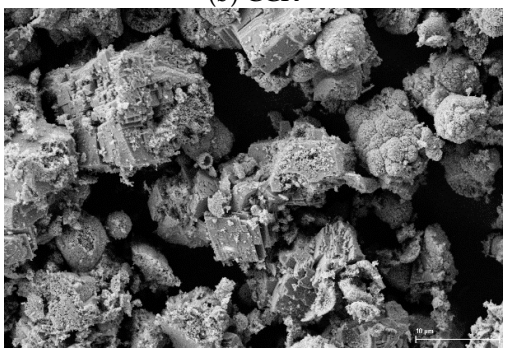

(d) CCNa

 doi:10.20944/preprints202602.1618.v1

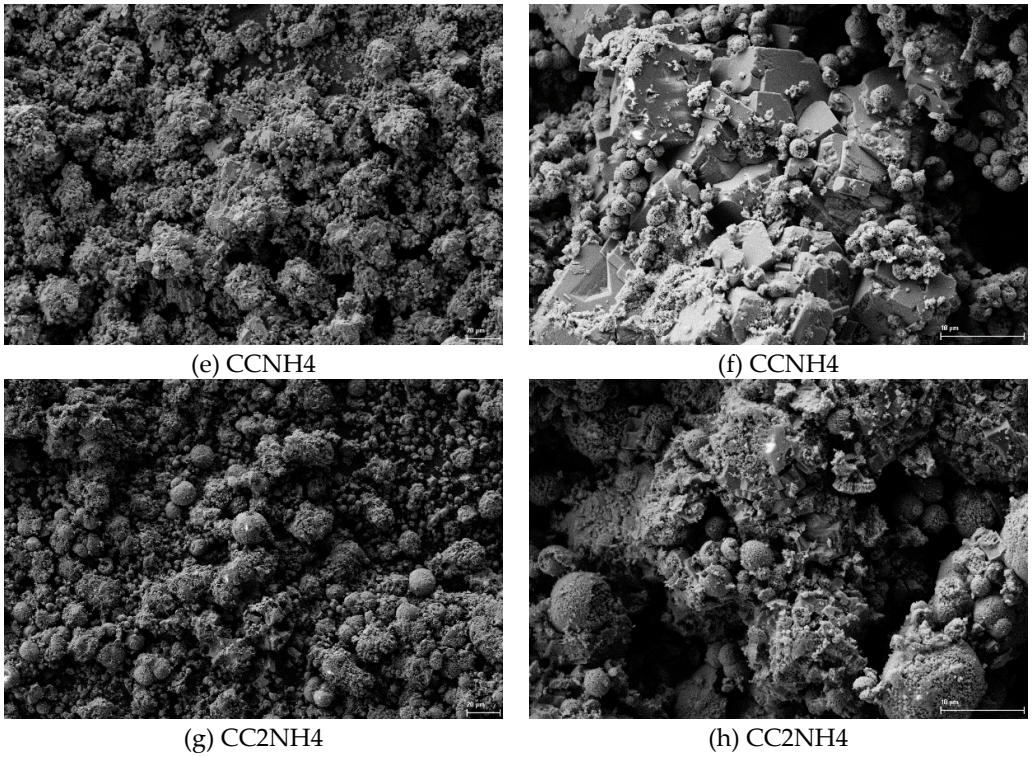

(e) CCNH4 (f) CCNH4

(g) CC2NH4 (h) CC2NH4

Figure 9. SEM images of synthesized powders CCK (a, b), CCNa (c, d), CCNH4 (e, f), CC2NH4 (g, h) at different magnification x1000, bar scale=20µm (a, c, e, g – left column) and x5000, bar scale =10µm (b, d, f, h – right column).

The mass loss for powders CCNH4 and CC2NH4 also take place in the interval from 100 °C to 600 °C due to decomposition of NH_4Cl (reaction 7) and $(NH_4)_2CO_3$ (reaction 8).

$$NH_4Cl \rightarrow NH_3\uparrow + HCl\uparrow \quad (7)$$

$$(NH_4)_2CO_3 \rightarrow 2NH_3\uparrow + CO_2\uparrow + H_2O\uparrow \quad (8)$$

Ammonium chloride NH_4Cl and ammonium carbonate $(NH_4)_2CO_3$ undergo thermal degradation in the lower temperature range: $(NH_4)_2CO_3$ decomposes with the release of $2NH_3$ and CO_2 already at temperatures below 60 °C, and NH_4Cl dissociates into NH_3 and HCl in the range of 300-350 °C. HCl formed during heating can react with $CaCO_3$ with $CaCl_2$ formation (reaction 9).

$$2HCl + CaCO_3 \rightarrow CaCl_2 + CO_2 \quad (9)$$

Or probably $CaCO_3$ even can interact with melt of NH_4Cl with $CaCl_2$ formation (reaction 10).

$$2NH_4Cl + CaCO_3 \rightarrow CaCl_2 + CO_2 + NH_3 \quad (10)$$

Theoretically possible mass loss due to $CaCO_3$ decomposition according to reaction (6) is 44% [60]. So, addition mass loss can be explained with presence of salts adsorbed and occluded from mother liquor in synthesized powder. It is worth to note that after calcium carbonate decompositions TG curves reflect the continuation of mass loss. Presence of KCl (CCK), NaCl (CCNa) and $CaCl_2$ (CCNH4 and CC2NH4) in the powders can be a reason of mass after $CaCO_3$ decomposition due to their ability to evaporate above the temperature of melting point 776 °C (KCl), 801 °C (NaCl), and 772 °C ($CaCl_2$).

Densities of prepared suspensions of calcium carbonate powders in aqueous solution of sodium alginate (Table 4) slightly diminish in the row: AlgNa_CCK, AlgNa_CCNa, AlgNa_$CCNH_4$, AlgNa_$CC2NH_4$.

 doi:10.20944/preprints202602.1618.v1

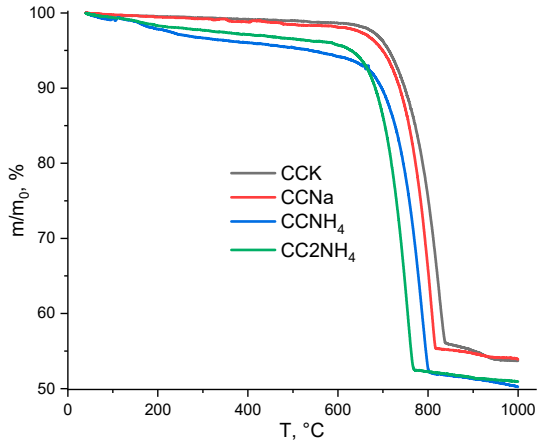

Figure 10. Thermal analysis data of powders synthesized from different pairs of precursors.

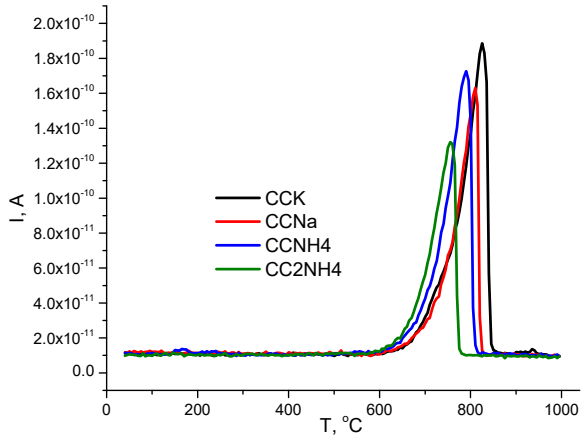

Figure 11. MS-spectra of data of powders synthesized from different pairs of precursors for m/z=44 (CO_2).

Table 4. Density of suspensions of calcium carbonate powders in aqueous solution of sodium alginate.

Suspension	Density of suspension, g/cm³
AlgNa	0,94
AlgNa_CCK	1,11
AlgNa_CCNa	1,09
AlgNa_CCNH4	1,01
AlgNa_CC2NH4	0,95

A decrease in density is observed in suspensions AlgNa_CCNH4, AlgNa_CC2NH4 prepared from powders $CaCO_3$ containing ammonium carbonate and ammonium chloride as reaction by-product. This decrease is directly related to the decomposition of ammonium carbonate with the release of gaseous products of ammonia and carbon dioxide according to reaction (8). Thus, the low density of suspension AlgNa_CC2NH4 containing $(NH_4)_2CO_3$ can be explained by the presence of dispersed air bubbles in their volume. These bubbles are the result of two possible processes: capture of gases released during decomposition of $(NH_4)_2CO_3$ in the case of appropriate suspensions, and/or mechanical entrainment of air into a highly viscous polymer medium during sample preparation, which is especially typical for a pure alginate solution or for suspensions AlgNa_CCK and AlgNa_CCNa. Since the density of the gas phase is three orders of magnitude lower than the density of liquid and solid particles, even a small volume of entrained gas leads to a significant decrease in the apparent (average) density of the entire heterogeneous system. Consequently, suspension

 doi:10.20944/preprints202602.1618.v1

AlgNa_CC2NH$_4$ with (NH$_4$)$_2$CO$_3$ is three-phase (solid-liquid-gas) systems, where the presence of gas inclusions is the dominant factor determining their density. Solution of pure alginate at the initial stage of homogenization is two-phase (solid-liquid) system. Low density of solution of pure sodium alginate also can be explained by the absence of the solid (powders of CaCO$_3$).

For an indirect comparative assessment of the rheological properties of the studied suspensions, the spreading area analysis method was applied. The technique is based on the relationship between the viscosity of a liquid and the diameter of the spot it forms when spreading under the influence of gravity on a horizontal surface (Table 5, Figure 5).

Table 5. Estimation of spreading area of suspensions of calcium carbonate powders in aqueous solution of sodium alginate.

Suspension	The spreading area of suspensions, cm^2
AlgNa_CCK	52
AlgNa_CCNa	65
AlgNa_CCNH$_4$	48
AlgNa_CC2NH$_4$	46

This method is relative and allows the ranking of samples according to their effective viscosity: a smaller spreading area with the same sample weight indicates a higher structural resistance to flow, that is, a higher viscosity.

With an exception of AlgNa_CC2NH4, suspensions show increase in viscosity corresponding to vaterite phase content increase in the phase composition of calcium carbonate powders used as fillers (Figure 12). The rheological curves of suspensions AlgNa_CCK and AlgNa_CCNa with calcium carbonate synthesized from sodium and potassium carbonates, as well as the curve of a pure sodium alginate solution, turned out to be very close in values and occupied an intermediate position.

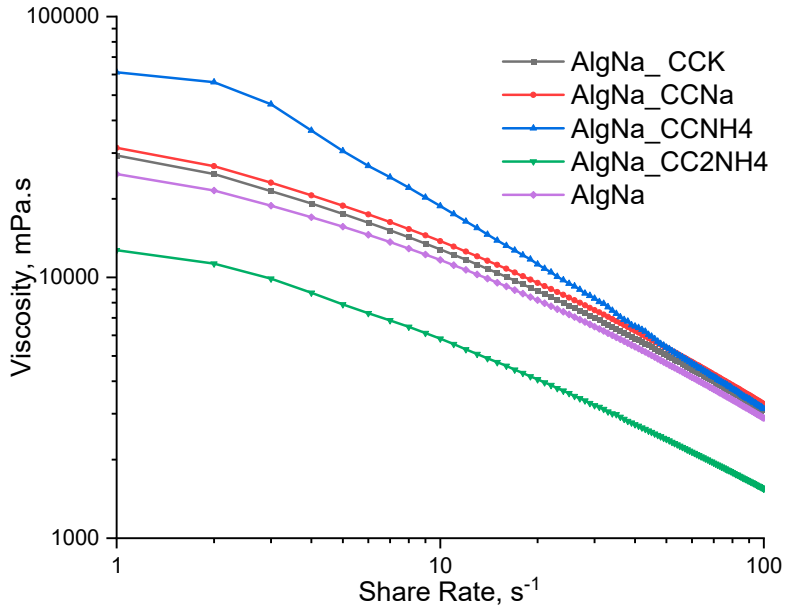

Figure 12. Dependence of viscosity of suspensions under investigation from the share rate.

AlgNa_CCNH4 suspension shows the highest viscosity values in the entire studied range of shear rates. Great viscosity increase at lower shear rates can be due to possible ionic crosslinking of sodium alginate. Traces of ammonium chloride, soluble by-product (reaction 11), being at first adsorbed on the surface of vaterite and calcite crystals from mother liquor may then dissolve into

 doi:10.20944/preprints202602.1618.v1

water of suspension and provoke $CaCO_3$ dissolution via soluble $CaCl_2$ formation (reaction 12). Presence of Ca^{2+} ions in suspension reacting with sodium alginate replacing some sodium cations and providing possibility of partial cross-linking of alginate.

$$NH_4Cl \rightarrow NH_4^+ + Cl^- \quad (11)$$

$$2NH_4^+ + 2Cl^- + CaCO_3 \rightarrow CaCl_2 + (NH_4)_2CO_3 \quad (12)$$

On the contrary, a suspension AlgNa_CC2NH4 with calcium carbonate obtained in presence of excess of $(NH_4)_2CO_3$ showed the lowest viscosity. Abnormal rheological properties of suspension filled with CC2NH4 can be possibly explained by presence of gas bubbles, created by decomposition of ammonium carbonate excess precursor that was adsorbed on the surface of vaterite crystals from the traces of mother liquor remaining on filtered crystals. Presence of gas bubbles in the suspension AlgNa_CC2NH4 can a reason of the lowest viscosity in comparison with the other suspensions under investigation.

Indirect test of suspensions properties (Figure 6) further confirm that crosslinking is happening in suspension filled with CCNH4 and CC2NH4 powders showing increased hygroscopicity and water retention, and their puddles having uneven form while AlgNa_CCK, AlgNa_CCNa suspensions and alginate solution puddles are lens-like flat puddle.

A notable feature is the behavior of rheological curves at high shear rates: the curve for a suspension AlgNa_CCNH4 asymptotically approaches and merges with a group of curves for suspension AlgNa_CCK, AlgNa_CCNa and AlgNa, while the curve for suspension AlgNa_CC2NH4 remains parallel to them, without showing tendencies to merge.

The key factors are the surface charge of calcium carbonate particles, their tendency to agglomerate, and, as a result, the effective volume of the dispersed phase, which determines the viscosity. The high viscosity of the suspension AlgNa_CCNH4 indicates the formation of a volumetric spatial structure in the system. The surface of the $CaCO_3$ particles probably has a charge close to the isoelectric point, which minimizes electrostatic repulsion between the particles. This contributes to their aggregation and the formation of large, loose floccules, which effectively bind a large amount of the dispersion medium (alginate solution) and create a strong framework that dramatically increases viscosity. The convergence of this curve with others at high shear rates is a classic sign of thixotropic behavior - the destruction of the structure under the action of shear deformation.

On the contrary, the viscosity is low and the curve runs parallel for a system with an abundance of carbonate ions (AlgNa_CC2NH4) indicate the presence of a well-peptised, stabilized system. Under these conditions, the surface of $CaCO_3$ particles acquires a significant negative charge due to the adsorption of excess CO_3^{2-} ions. Since alginate macromolecules also carry a negative charge, electrostatic repulsion occurs between particles and polymer chains. This prevents agglomeration and promotes the uniform distribution of individual, stabilized particles in the volume. Such a system does not form a solid structure, its viscosity is determined mainly by the viscosity of the polymer matrix and varies slightly with shear rate, which explains the parallel course of the curve. Similar viscosity values for systems with sodium and potassium carbonates, as well as pure alginate, suggest that $CaCO_3$ particles obtained by these methods also have good colloidal stability and do not significantly contribute to structure formation, their behavior approaches that of a filler in a Newtonian fluid.

The analysis of the drying process of suspensions containing synthesized calcium carbonates and small quantities of reaction by-products revealed the exponential nature of the mass changes over time (Figure 13).

 doi:10.20944/preprints202602.1618.v1

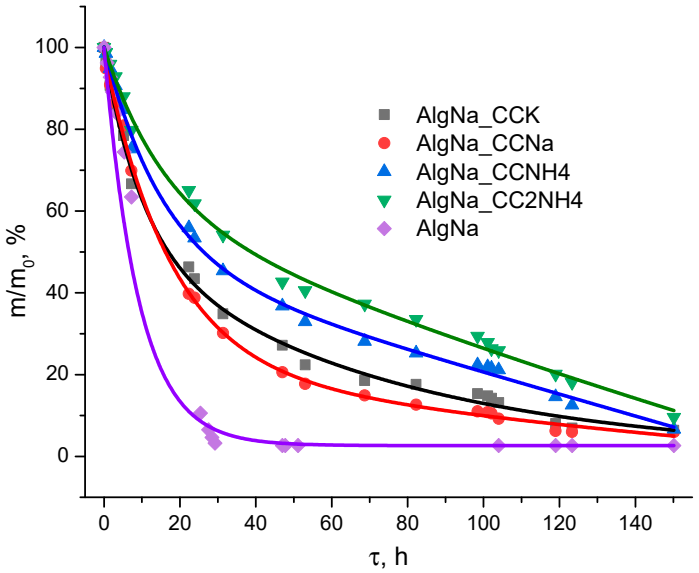

Figure 13. The mass-time dependence for suspensions calcium carbonate powders synthesized from different pairs of precursors in aqueous solution of sodium alginate.

At the same time, it was found that suspensions formulated on the basis of calcium carbonate powders obtained from ammonium carbonates are characterized by a statistically significantly lower drying rate compared with compositions based on powders obtained from potassium and sodium carbonates.

The key reason is the presence of significant amounts of hygroscopic ammonium salts in these systems, primarily ammonium chloride (NH_4Cl) and possibly residual ammonium carbonate ($(NH_4)_2CO_3$). The results were influenced by reaction byproducts, but their presence were determined only indirectly. These compounds have a pronounced ability to sorption of moisture from the atmosphere and retain it in the form of hydrate shells, which increases the total content of bound liquid in the sample volume.

In addition, hydrated ammonium ions NH_4^+ and chloride ions Cl^-, sorbed on the surface of calcium carbonate particles, can form stable hydrate layers, increase the binding energy of the "solid phase" and complicate its removal.

Thus, the delayed kinetics of drying suspensions based on CCNH4 and CC2NH4 powders is a consequence of the action of two main mechanisms: first, the physico-chemical retention of moisture by hygroscopic ammonium salts, and, secondly, the formation of a thinner porous structure that increases capillary forces and the path for the diffusion of water vapor. In suspensions based on powders of CCK and CCNa with non-hygroscopic chlorides as by-products these factors are absent, and this causes their higher rate of dehydration.

The obtained XRD (Figure 14) and FTIR (Figure 15) data for composites demonstrate full consistency with the results of the analysis of the calcium carbonate powders after synthesis. This clearly indicates that the process of introducing powders into the polymer matrix of alginate, subsequent cross-linking of polymer and cryogenic drying do not induce phase transitions of polymorphic modifications of calcium carbonate and do not change their initial phase composition.

 doi:10.20944/preprints202602.1618.v1

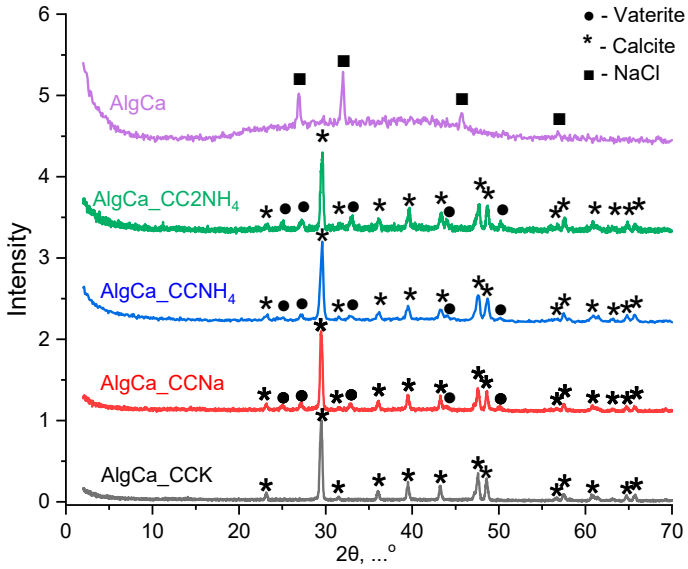

Figure 14. XRD data of composites with CaAlg matrix and synthesized $CaCO_3$ powders: • — vaterite (PDF No 33-268; No 96-900-7476); * —calcite (PDF No 5-586; No 96-900-0096);
■ – NaCl (PDF No 72-1668; No 96-100-0042).

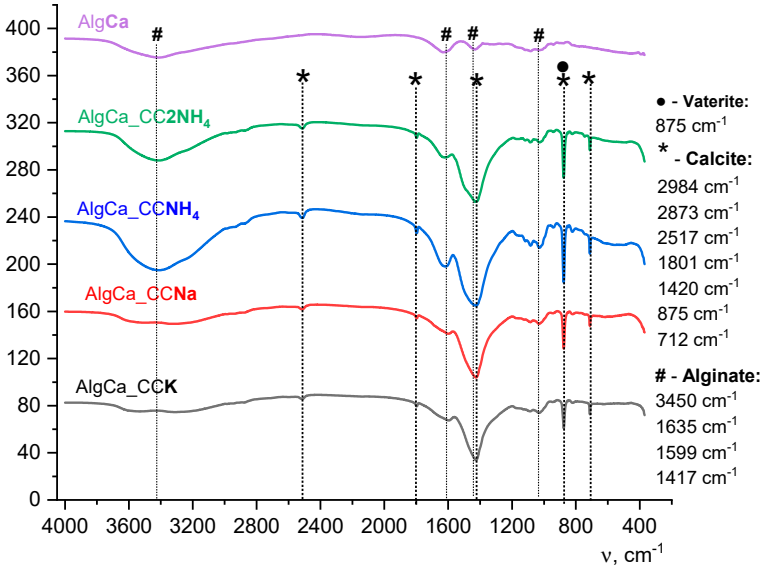

Figure 15. FTIR spectra of composites with CaAlg matrix and synthesized $CaCO_3$ powders as a filler after frees drying.

According to XRD and FTIR data, the initial phase composition is preserved in all studied composite materials. In the composites based on a CCK powder calcium carbonate is present exclusively in the form of a thermodynamically stable modification of calcite. Its FTIR spectrum is characterized by a doublet in the region of δ vibrations ~710 cm^{-1}, and the diffraction pattern contains reflections unique to the rhombohedral structure of calcite. On the contrary, in composites containing powders CCNa, CCNH4 and CC2NH4, a two-phase system is identified (Figure 14). Along with the calcite reflections, the diffractograms show peaks corresponding to the metastable hexagonal phase of vaterite. This is reliably confirmed by FTIR spectroscopy data, where in the spectra of these

 doi:10.20944/preprints202602.1618.v1

samples, along with the bands of calcite, a characteristic sharp absorption band of vaterite in the region of ~875 cm^{-1} is observed.

This confirms the stability of polymorphic modifications of calcium carbonate within the framework of the applied technique for obtaining composite materials and proves the representativeness of the analysis of the powders themselves for predicting the composition and structure of the final composite systems.

The calcium carbonate in the initial system performs the function of a source of divalent cations with delayed release. The dissolution of calcium carbonate particles with the release of Ca^{2+} ions, which interact with the carboxyl groups of alginate chains, forming transverse ionic bonds. The coacervation of polymer chains and increased intermolecular interactions, further stabilizing the three-dimensional grid.

Photos made using optical microscope of composites with CaAlg matrix and synthesized $CaCO_3$ powders as a filler in form of meshes presented at Figure 16. These photos confirm the quite uniform distribution of filler particles in the polymer matrix for AlgCa_CCK and AlgCa_CCNa meshes. In the contrary photos of AlgCa_CCNH4 and AlgCa_CC2NH4 meshes gives opportunity to see their non homogenous structure with presence of gas babbles and particles big aggregates.

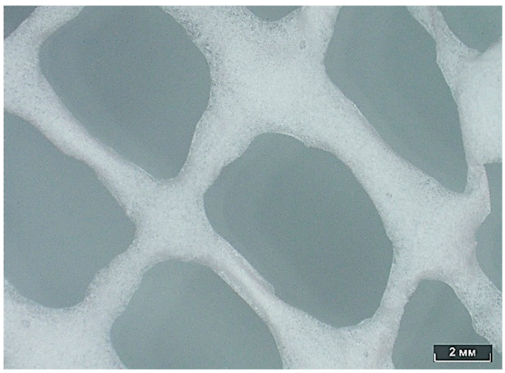

AlgCa_CCK (a)

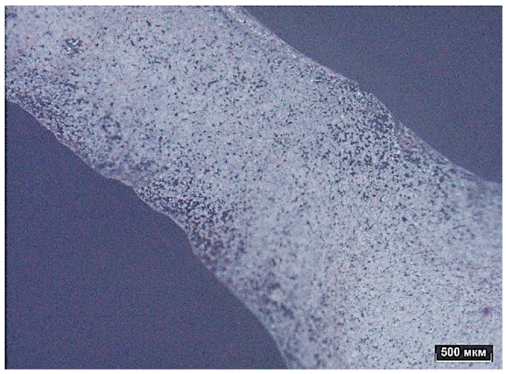

AlgCa_CCK (b)

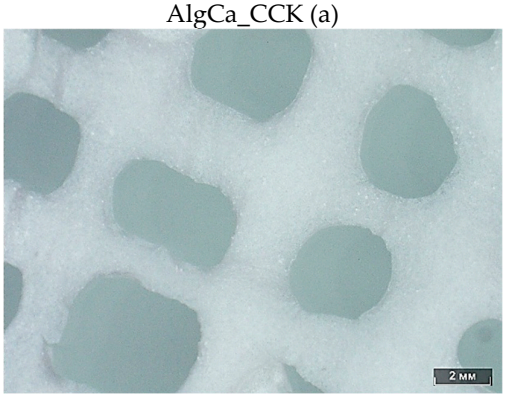

AlgCa_CCNa (c)

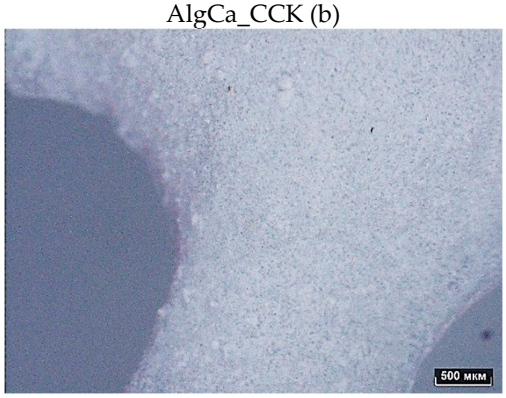

AlgCa_CCNa (d)

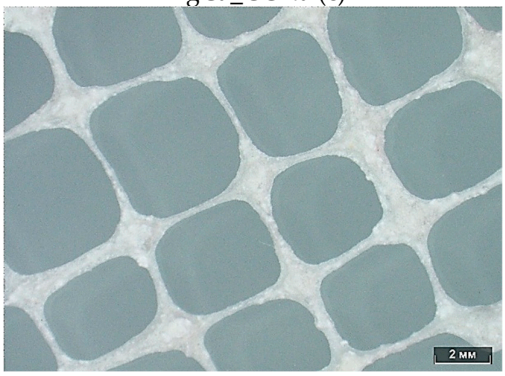

AlgCa_CCNH4 (e)

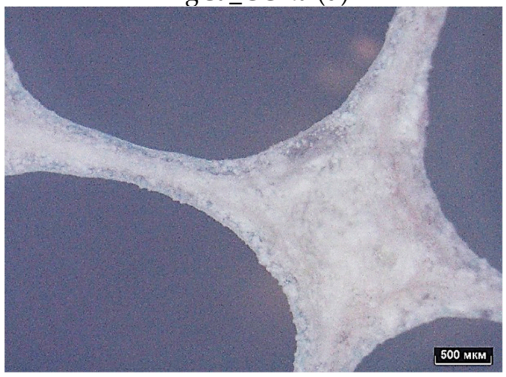

AlgCa_CCNH4 (f)

 doi:10.20944/preprints202602.1618.v1

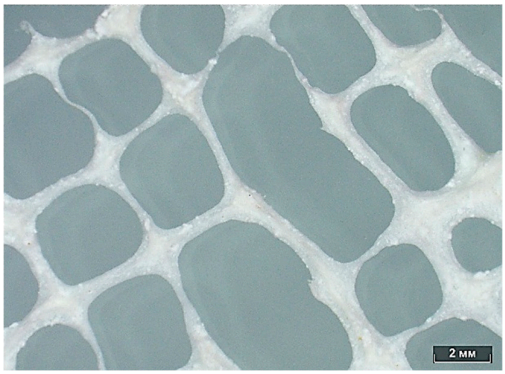

AlgCa_CC2NH4 (g)

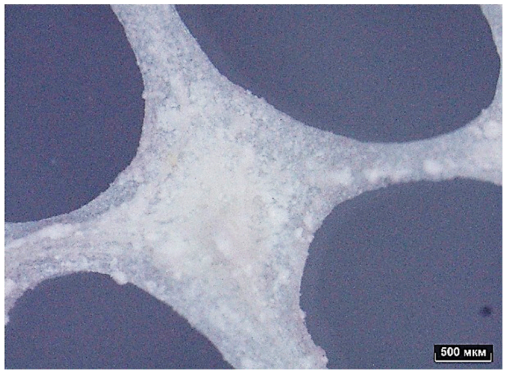

AlgCa_CC2NH4 (h)

Figure 16. Photos made using optical microscope of composites with CaAlg matrix and synthesized $CaCO_3$ powders: AlgCa_CCK (a, b), AlgCa_CCNa (c, d), AlgCa_CCNH4 (e , f), AlgCa_CC2NH4 (g, h) at different magnification.

SEM images of surfaces of films presented at Figure 17. It worth to note that alginate cross-linking during preparation of the films cause their strong deformation (Figure 4). SEM images of surfaces give opportunity to estimate forms of filler's particles in the composite under the layer of polymer. Surface terrain of composite films is influenced by filler particle's shape. The forms of $CaCO_3$ particle in the polymer matrix course recollection of forms of particles of synthesized powders which can be seen at their SEM images (Figure 9).

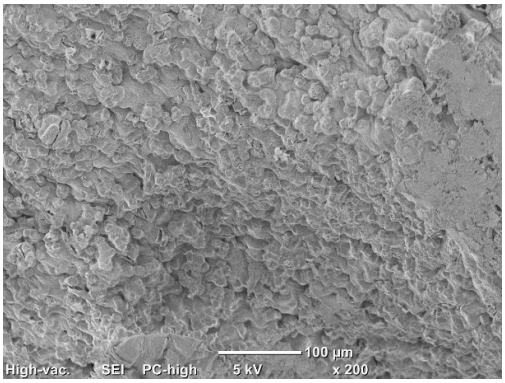

AlgCa_CCK (a)

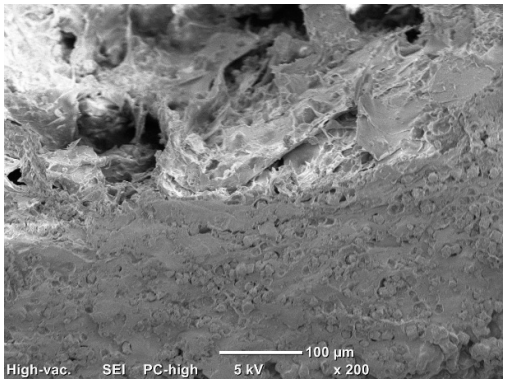

AlgCa_CCNa (b)

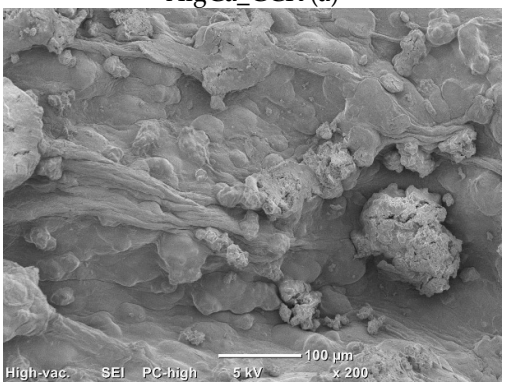

AlgCa_CCNH4 (c)

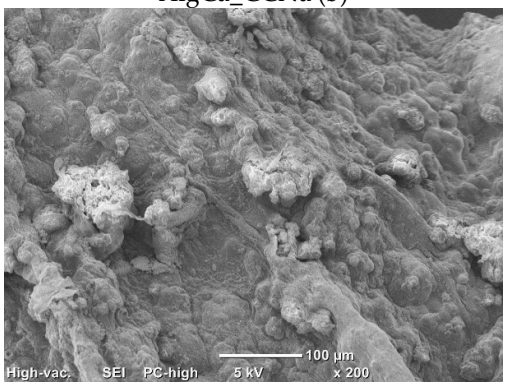

AlgCa_CC2NH4 (d)

Figure 17. SEM images of composites with CaAlg matrix and synthesized $CaCO_3$ powders: AlgCa_CCK (a), AlgCa_CCNa (b), AlgCa_CCNH4 (c), AlgCa_CC2NH4 (d).

 doi:10.20944/preprints202602.1618.v1

4. Conclusions

Strategy of preparation of composite materials with alginate matrix and $CaCO_3$ filler included $CaCO_3$ powder synthesis; suspension of powder in aqueous solution of sodium alginate homogenization; granules, meshes and films formation via $CaCl_2$ cross-linking; and freeze drying under deep vacuum.

Different pair of precursors, i.e. $K_2CO_3/CaCl_2$, $Na_2CO_3/CaCl_2$, $(NH_4)_2CO_3/CaCl_2$, and $2(NH_4)_2CO_3/CaCl_2$ were used for $CaCO_3$ synthesis. Solution of soluble carbonates used for synthesis having basic pH provided the formation of thermodynamically stable calcite in all powders. Presence of ammonium ion in reaction zone helped the vaterite formation. The highest content of metastable vaterite was in the $CaCO_3$ powder synthesized at molar ratio Ca/CO_3=0.5 from aqueous solutions of calcium chloride and ammonium carbonate taken in excess.

Preservation of reaction by-products in the synthesized powders of calcium carbonate even in the small quantities can be treated as an effective tool of reaching target properties of powders, suspensions and composite materials. Suspension based on powder of $CaCO_3$ with phase composition presented by calcite and vaterite containing NH_4Cl as reaction by-product demonstrated the maximum viscosity values due to the possible cross-liking reaction during the suspension preparation. On the contrary, a suspension based on powder of $CaCO_3$ with phase composition presented by calcite and vaterite containing NH_4Cl as reaction by-product and $(NH_4)_2CO_3$ has the lowest viscosity due to the presence of babbles of gas phase.

The presence of ammonium salts (NH_4Cl, $(NH_4)_2CO_3$) in the suspensions based of powders of $CaCO_3$ influenced on the process of their drying at room temperature delaying the mass loss. It was confirmed that phase composition of $CaCO_3$ powders used as a filler remain stable during creation of composites with alginate matrix.

Created composite materials in form of granules, meshes and films based on Ca-cross-linked alginate and powders of synthetic calcium carbonate can be recommended for the skin wounds and bone defects treatment, and drug carriers.

Author Contributions: Conceptualization, M.M.A., T.V.S., N.R.K.; methodology, M.M.A., T.V.S., N.R.K.; investigation, M.M.A., T.V.S., A.A.P., O.A.K., T.B.S., V.B.P., A.M.M., Y.Y.F., E.A.M., O.T.G., O.V.B., A.C., A.V.K., N.R.K.; resources, T.B.S., V.B.P., Y.Y.F., O.T.G., O.V.B.; writing—original draft preparation, M.M.A., T.V.S., A.A.P., O.A.K.; writing—review and editing, M.M.A., T.V.S., N.R.K.; visualization, M.M.A., A.A.P., O.A.K., E.A.M., A.M.M., O.T.G., O.V.B.; supervision, T.V.S., N.R.K.; project administration, T.V.S., N.R.K.; All authors have read and agreed to the published version of the manuscript.

Funding: This work was carried out with the support of the State assignment of the Lomonosov Moscow State University: AAAA-A21-121011590082-2 and with the support of the State assignment of the Lomonosov Moscow State University: № 121031300090-2.

Data Availability Statement: All research data presented in the article.

Acknowledgments: This research was carried out using the equipment of the MSU Shared Research Equipment Center “Technologies for obtaining new nanostructured materials and their complex study” and was purchased by MSU within the framework of the Equipment Renovation Program (National Project “Science”) and within the framework of the MSU Program of Development. Authors would like to acknowledge the Company Lukon Pro (www.lucon.pro) and Alexey Monakov for providing opportunity of samples microstructure investigation.

Conflicts of Interest: The authors declare no conflicts of interest.

 doi:10.20944/preprints202602.1618.v1

References

1. Venkatesan, J.; Bhatnagar, I.; Manivasagan, P.; Kang, K.H.; Kim, S.K. Alginate composites for bone tissue engineering: A review. *Int. J. Biol. Macromol.*, **2015,** 72, 269-281. https://doi.org/10.1016/j.ijbiomac.2014.07.008
2. Hasnain, M.S.; Nayak, A.K. Alginate-inorganic composite particles as sustained drug delivery matrices. In *Applications of Nanocomposite materials in drug delivery* Edited by: Inamuddin, Abdullah M. Asiri and Ali Mohammad Eds.; Woodhead Publishing, 2018, pp. 39-74. https://doi.org/10.1016/B978-0-12-813741-3.00003-0
3. Zhang, M.; Zhao, X. Alginate hydrogel dressings for advanced wound management. *Int. J. Biol. Macromol.* **2020**, *162,* 1414–1428. https://doi.org/10.1016/j.ijbiomac.2020.07.311
4. Smidsrød, O.; Skjak-Bræk, G. Alginates as immobilization matrix for cells. *Trends Bio-technol.* **1990**, *8(1),* 71–78. https://doi.org/10.1016/0167-7799(90)90139-o
5. Tomić, S.L.; Babić Radić, M.M.; Vuković, J.S.; Filipović, V.V.; Nikodinovic-Runic, J.; Vukomanović, M. Alginate-Based Hydrogels and Scaffolds for Biomedical Applications. *Mar. Drugs* **2023**, *21*, 177. https://doi.org/10.3390/md21030177
6. Varaprasad K, Jayaramudu T, Kanikireddy V, Toro C, Sadiku ER. Alginate-based composite materials for wound dressing application: A mini review. *Carbohydr Polym*. 2020; 236:116025. https://doi.org/10.1016/j.carbpol.2020.116025
7. Wang, B.; Wan, Y.; Zheng, Y.; Lee, X.; Liu, T.; Yu, Z.; Huang, J.; Sik Ok, Y.; Chen, B.; Gao, B. Alginate-based composites for environmental applications: a critical review. *Crit. Rev. Environ. Sci Technol.* **2019**, *49(4),* 318-356. https://doi.org/10.1080/10643389.2018.1547621
8. Thakur, S. An overview on alginate based bio-composite materials for wastewater remedial. *Materials today*: *proceedings*, **2021**. 37, 3305-3309. https://doi.org/10.1016/j.matpr.2020.09.120
9. Omer, S. (2021). Heavy metal removal by alginate based agriculture and industrial waste nanocomposites. In *Properties and Applications of Alginates*. IntechOpen. Deniz, Irem (editor), Imamoglu, Esra (editor), Keskin-Gundogdu, Tugba (editor) Properties and Applications of Alginates | IntechOpen https://doi.org/10.5772/intechopen.98832
10. Tsyganova, A.A.; Golovanova, O.A. Synthesis of a Composite Material Based on a Mixture of Calcium Phosphates and Sodium Alginate. *Inorg Mater* **2019,** *55,* 1156–1161 https://doi.org/10.1134/S0020168519110141
11. Alharaty, G.; Ramaswamy, H.S. The Effect of Sodium Alginate-Calcium Chloride Coating on the Quality Parameters and Shelf Life of Strawberry Cut Fruits. *J. Compos. Sci.* **2020**, *4*, 123. https://doi.org/10.3390/jcs4030123
12. Augst, A.D.; Kong, H.J.; Mooney, D.J. Alginate hydrogels as biomaterials. Macromol. Biosci. 2006, 6(10), 663–673 https://doi.org/10.1002/mabi.200600069
13. Elango, J.; Zamora-Ledezma, C.; Maté-Sánchez de Val, J.E. Natural vs Synthetic Polymers: How Do They Communicate with Cells for Skin Regeneration—A Review. *J. Compos. Sci.* **2023**, *7*, 385. https://doi.org/10.3390/jcs7090385
14. George M, Abraham TE. Polyionic hydrocolloids for the intestinal delivery of protein drugs: alginate and chitosan--a review. *J. Control. Release.* **2006**, *114(1)*, 1-14. https://doi.org/10.1016/j.jconrel.2006.04.017
15. Lee, K.Y.; Mooney, D.J. Alginate: properties and biomedical applications. *Prog. Polym. Sci.* **2012,** *37(1)*, 106–126. https://doi.org/10.1016/j.progpolymsci.2011.06.003
16. Martinsen, A.; Skjak-Bræk, G.; Smidsrød, O. Alginate as immobilization material: I. Correlation between chemical and physical properties of alginate gel beads. *Biotechnol. Bioeng.* **1989,** *33(1),* 79–89. https://doi.org/10.1002/bit.260330111
17. Hurtado, A.; Aljabali, A.A.A.; Mishra, V.; Tambuwala, M.M.; Serrano-Aroca, Á. Alginate: Enhancement Strategies for Advanced Applications. *Int. J. Mol. Sci.* **2022**, *23*, 4486. https://doi.org/10.3390/ijms23094486
18. Zueva, O.S.; Khair, T.; Derkach, S.R.; Kazantseva, M.A.; Zuev, Y.F. Strontium-Induced Gelation of Sodium Alginate in the Presence of Carbon Nanotubes: Elemental Analysis and Gel Structure. *J. Compos. Sci.* **2023**, *7*, 286. https://doi.org/10.3390/jcs7070286

 doi:10.20944/preprints202602.1618.v1

19. Wurm, F.; Rietzler, B.; Pham, T.; Bechtold, T. Multivalent Ions as Reactive Crosslinkers for Biopolymers—A Review. *Molecules* **2020**, *25*, 1840. https://doi.org/10.3390/molecules25081840
20. Zhou Q, Kang H, Bielec M, et al. Influence of different divalent ions cross-linking sodium alginate-polyacrylamide hydrogels on antibacterial properties and wound healing. *Carbohydr Polym.* **2018,** *197,* 292-304. https://doi.org/10.1016/j.carbpol.2018.05.078
21. Ručigaj, A.; Golobič, J.; Kopač, T. The role of multivalent cations in determining the cross-linking affinity of alginate hydrogels: A combined experimental and modeling study. *Chem. Eng. J. Adv.* **2024,** 20, 100678. https://doi.org/10.1016/j.ceja.2024.100678
22. Massana Roquero D., Othman A., Melman A., Katz E. Iron(iii)-cross-linked alginate hydrogels: a critical review. *Mater. Adv.* **2022,** *3(4)*. 1849-1873. https://xlink.rsc.org/?DOI=D1MA00959A
23. Makarova, A.O.; Derkach, S.R.; Khair, T.; Kazantseva, M.A.; Zuev, Y.F.; Zueva, O.S. Ion-Induced Polysaccharide Gelation: Peculiarities of Alginate Egg-Box Association with Different Divalent Cations. *Polymers* **2023**, *15*, 1243. https://doi.org/10.3390/polym15051243
24. Tiwari, A.; Jain, A.; Verma, A.; Panda, P.K.; Jain, S.K. Alginate-based composites in drug delivery applications. In *Alginates,* 1st ed.; Md Saquib Hasnain, Amit Kumar Nayak Eds.; Apple Academic Press, New York, USA, 2019, pp. 457-482 https://doi.org/10.1201/9780429023439
25. Bibi, A.; Rehman, S.U.; Yaseen, A. Alginate-nanoparticles composites: kinds, reactions and applications. *Mater. Res. Express* **2019,** *6(9)*, 092001. https://doi.org/10.1088/2053-1591/ab2016
26. Kvesitadze, G.I.; Graves, D.J. Calcium alginate/magnetite spheres: a new support for chromatographic separations and enzyme immobilization. *Biotechnol. Bioeng.* **1985,** *27(2),* 137–145. https://doi.org/10.1002/bit.260270206
27. Shabadrov, P.A.; Safronov, A.P.; Kurilova, N.M.; Blyakhman, F.A. Design of Spherical Gel-Based Magnetic Composites: Synthesis and Characterization. *J. Compos. Sci.* **2023**, *7*, 177. https://doi.org/10.3390/jcs7050177
28. Gobi, R.; Ravichandiran, P.; Babu, R.S.; Yoo, D.J. Biopolymer and Synthetic Polymer-Based Nanocomposites in Wound Dressing Applications: A Review. *Polymers* **2021**, *13*, 1962. https://doi.org/10.3390/polym13121962
29. Alkaron, W.; Almansoori, A.; Balázsi, C.; Balázsi, K. A Critical Review of Natural and Synthetic Polymer-Based Biological Apatite Composites for Bone Tissue Engineering. *J. Compos. Sci.* **2024**, *8*, 523. https://doi.org/10.3390/jcs8120523
30. Hussin, M.S.F.; Mohd Serah, A.; Azlan, K.A.; Abdullah, H.Z.; Idris, M.I.; Ghazali, I.; Mohd Shariff, A.H.; Huda, N.; Zakaria, A.A. A Bibliometric Analysis of the Global Trend of Using Alginate, Gelatine, and Hydroxyapatite for Bone Tissue Regeneration Applications. *Polymers* **2021**, *13*, 647. https://doi.org/10.3390/polym13040647
31. Estevez, A.T.; Abdallah, Y.K. Biomimetic Approach for Enhanced Mechanical Properties and Stability of Self-Mineralized Calcium Phosphate Dibasic–Sodium Alginate–Gelatine Hydrogel as Bone Replacement and Structural Building Material. *Processes* **2024**, *12*, 944. https://doi.org/10.3390/pr12050944
32. Chen, X.; Wu, T.; Bu, Y.; Yan, H.; Lin, Q. Fabrication and Biomedical Application of Alginate Composite Hydrogels in Bone Tissue Engineering: A Review. *Int. J. Mol. Sci.* **2024**, *25*, 7810. https://doi.org/10.3390/ijms25147810
33. Sikkema, R.; Keohan, B.; Zhitomirsky, I. Alginic Acid Polymer-Hydroxyapatite Composites for Bone Tissue Engineering. *Polymers* **2021**, *13*, 3070. https://doi.org/10.3390/polym13183070
34. Hernández-González, A. C., Téllez-Jurado, L., & Rodríguez-Lorenzo, L. M. Alginate hydrogels for bone tissue engineering, from injectables to bioprinting: A review. *Carbohydrate polymers*, **2020.** *229*, 115514. https://doi.org/10.1016/j.carbpol.2019.115514
35. Sukhodub, L. F., Sukhodub, L. B., Litsis, O., & Prylutskyy, Y. (2018). Synthesis and characterization of hydroxyapatite-alginate nanostructured composites for the controlled drug release. *Materials Chemistry and Physics*, *217*, 228-234. https://doi.org/10.1016/j.matchemphys.2018.06.071
36. Merle, M., Lagarrigue, P., Wang, S., Duployer, B., Tenailleau, C., Muller, W. E., ... & Soulié, J. (2025). Freeze-cast composites of alginate/pyrophosphate-stabilized amorphous calcium carbonate: from the nanoscale structuration to the macroscopic properties. *ACS Biomater. Sci. Eng.* **2025,** *11*(2), 1198-1211. https://doi.org/10.1021/acsbiomaterials.4c01396

 doi:10.20944/preprints202602.1618.v1

37. Mahmood, Z.; Amin, A.; Zafar, U.; Raza, M.A.; Hafeez, I.; Akram, A. Adsorption studies of cadmium ions on alginate–calcium carbonate composite beads. *Appl. Water. Sci.* **2017.** *7*(2), 915-921. https://doi.org/10.1007/s13201-015-0302-2
38. Wang, B., Gao, B., Zimmerman, A. R., & Lee, X. (2018). Impregnation of multiwall carbon nanotubes in alginate beads dramatically enhances their adsorptive ability to aqueous methylene blue. *Chem. Eng. Research and Design*, *133*, 235-242. https://doi.org/10.1016/j.cherd.2018.03.026
39. Chen, Y.; Zhou, Y.; Wang, C. Investigation of Collagen-Incorporated Sodium Alginate Bioprinting Hydrogel for Tissue Engineering. *J. Compos. Sci.* **2022**, *6*, 227. https://doi.org/10.3390/jcs6080227
40. Hu, T.; Lo, A.C.Y. Collagen–Alginate Composite Hydrogel: Application in Tissue Engineering and Biomedical Sciences. *Polymers* **2021**, *13*, 1852. https://doi.org/10.3390/polym13111852
41. Marasinghe, W.N.; Jayathunge, K.G.L.R.; Dassanayake, R.S.; Liyanage, R.; Bandara, P.C.; Rajapaksha, S.M.; Gunathilake, C. Structure, Properties, and Recent Developments in Polysaccharide- and Aliphatic Polyester-Based Packaging—A Review. *J. Compos. Sci.* **2024**, *8*, 114. https://doi.org/10.3390/jcs8030114
42. Grigoraș, C.-G.; Simion, A.-I. Synthesis of a New Composite Material Derived from Cherry Stones and Sodium Alginate—Application to the Adsorption of Methylene Blue from Aqueous Solution: Process Parameter Optimization, Kinetic Study, Equilibrium Isotherms, and Reusability. *J. Compos. Sci.* **2024**, *8*, 402. https://doi.org/10.3390/jcs8100402
43. Priya, A.S.; Premanand, R.; Ragupathi, I.; Bhaviripudi, V.R.; Aepuru, R.; Kannan, K.; Shanmugaraj, K. Comprehensive Review of Hydrogel Synthesis, Characterization, and Emerging Applications. *J. Compos. Sci.* **2024**, *8*, 457. https://doi.org/10.3390/jcs8110457
44. Niculescu, A.-G.; Grumezescu, A.M. Applications of Chitosan-Alginate-Based Nanoparticles—An Up-to-Date Review. *Nanomaterials* **2022**, *12*, 186. https://doi.org/10.3390/nano12020186
45. Bi, Y.G.; Lin, Z.T.; Deng, S.T. Fabrication and characterization of hydroxyapatite/sodium alginate/chitosan composite microspheres for drug delivery and bone tissue engineering. *Mater. Sci. Eng. C Mater. Biol. Appl*. **2019.** https://doi.org/10.1016/j.msec.2019.03.040
46. Kucko, S. K., Raeman, S. M., & Keenan, T. J. (2023). Current advances in hydroxyapatite-and β-tricalcium phosphate-based composites for biomedical applications: a review. *Biomedical Materials & Devices*, *1*(1), 49-65. https://doi.org/10.1007/s44174-022-00037-w
47. Mosievich, D.V.; Balabushevich, N.G.; Mishin, P.I.; Filatova, L.Y.; Murina, M.A.; Pobeguts, O.V.; Galyamina, M.A.; Obraztsova, E.A.; Grigorieva, D.V.; Gorudko, I.V.; et al. Vaterite/Fucoidan Hybrid Microparticles: Fabrication, Loading of Lactoferrin, Structural Characteristics and Functional Properties. *Mar. Drugs* **2025,** 23, 428. https://doi.org/10.3390/md23110428
48. Wu D.H.; Preskitt C.; Gresham-Fiegel C. Chemical and Physiological Change from Calcium Carbonate to Calcium Phosphate in Skeletal Structures. *Insights Biomed. Res.* **2021,** *5(1),* 139- 148. https://doi.org/10.36959/584/460
49. Niu, Y.Q.; Liu, J.H.; Aymonier, C.; Fermani, S.; Kralj, D.; Falini, G.; Zhou, C.H. Calcium carbonate: controlled synthesis, surface functionalization, and nanostructured materials. *Chem. Soc. Rev.* **2022,** *51*(18), 7883-7943. https://doi.org/10.1039/D1CS00519G
50. Kralj, D.; Brečević, L. Dissolution kinetics and solubility of calcium carbonate monohydrate. *Colloids Surf. A: Physicochem. Eng. Asp.* **1995,** 96(3), 287-293. https://doi.org/10.1016/0927-7757(94)03063-6
51. Strohm, S. B., Saldi, G. D., Mavromatis, V., Schmahl, W. W., & Jordan, G. A study on ikaite growth in the presence of phosphate. *Aquatic Geochemistry*. **2023,** *29*(4), 219-233. https://doi.org/10.1007/s10498-023-09418-z
52. Merle, M., Soulié, J., Sassoye, C., Roblin, P., Rey, C., Bonhomme, C., & Combes, C. Pyrophosphate-stabilised amorphous calcium carbonate for bone substitution: toward a doping-dependent cluster-based model. *Cryst. Eng. Comm.* **2022,** *24(45)*, 8011-8026. https://doi.org/10.1039/D2CE00936F
53. Jimoh, O.A., Ariffin, K.S., Hussin, H.B. *et al.* Synthesis of precipitated calcium carbonate: a review. *Carbonates Evaporites*. **2018,** *33*, 331–346. https://doi.org/10.1007/s13146-017-0341-x
54. Chang, R.; Kim, S.; Lee, S.; Choi, S.; Kim, M.; Park, Y. Calcium carbonate precipitation for CO2 storage and utilization: a review of the carbonate crystallization and polymorphism. *Front. Energy Res.*, **2017.** *5*, 17. https://doi.org/10.3389/fenrg.2017.00017

 doi:10.20944/preprints202602.1618.v1

55. Declet, A., Reyes, E., & Suárez, O. M. (2016). Calcium carbonate precipitation: a review of the carbonate crystallization process and applications in bioinspired composites. *Rev. Adv. Mater. Sci.*, **2016,** *44(1),* 87-107. https://www.scopus.com/pages/publications/84962528365
56. Mihai, M.; Lotos, E.D.; Zaharia, M.M.; Bucatariu, F.; Vasiliu, A.L. Alginate-based Composite Hydrogels Formed by In Situ $CaCO_3$ Crystallization. *Cryst. Growth Des.* **2024**, *24, 6,* 2514–2525. https://doi.org/10.1021/acs.cgd.3c01518
57. Konopacka-Łyskawa, D. Synthesis Methods and Favorable Conditions for Spherical Vaterite Precipitation: A Review. *Crystals* **2019**, *9*, 223. https://doi.org/10.3390/cryst9040223
58. Bahrom, H.; Goncharenko, A.A.; Fatkhutdinova, L.I.; Peltek, O.O.; Muslimov, A.R.; Koval, O.Y.; Eliseev I.E., Manchev A., Gorin D., Shishkin I.I., Noskov R.E., Timin A.S., Ginzburg P., Zyuzin, M.V. Controllable synthesis of calcium carbonate with different geometry: comprehensive analysis of particle formation, cellular uptake, and biocompatibility. *ACS Sustain. Chem. Eng.*, **2019,** 7(23), 19142-19156. https://doi.org/10.1021/acssuschemeng.9b05128
59. ICDD (2010). PDF-4+ 2010 (Database), edited by Dr. Soorya Kabekkodu, International Centre for Diffraction Data. Newtown Square. PA. USA. http://www.icdd.com/products/pdf2.htm
60. Safronova, T.V.; Le, H.M.N.; Shatalova, T.B.; Murashko, A.M.; Filippova, T.V.; Motorin, E.A.; Tsymbarenko, D.M.; Golubchikov, D.O.; Boytsova, O.V.; Knotko, A.V. Powders Synthesized from Calcium Chloride and Mixed-Anionic Solution Containing Orthophosphate and Carbonate Ions. *Compounds* **2025**, *5*, 41. https://doi.org/10.3390/compounds5040041